Journal of Solid State Chemistry 182 (2009) 3118–3124

Contents lists available at ScienceDirect

Journal of Solid State Chemistry

journal homepage: www.elsevier.com/locate/jssc

Preparation, crystal structure and luminescent properties of the (6,3) type network supramolecular lanthanide picrate complexes with 2,2′-[(1,2-naphthalene)bis(oxy)]bis[N-(phenylmethyl)]acetamide

Qin Wang, Kuan-Zhen Tang, Wei-Sheng Liu, Yu Tang *, Min-Yu Tan

College of Chemistry and Chemical Engineering, State Key Laboratory of Applied Organic Chemistry, Lanzhou University, Lanzhou 730000, PR China

ARTICLE INFO

Article history:
Received 7 July 2009
Received in revised form
2 September 2009
Accepted 6 September 2009
Available online 11 September 2009

Keywords:
Lanthanide picrate complexes
Podand
Supramolecular structure
Luminescent properties

ABSTRACT

Solid complexes of lanthanide picrates with a new podand-type ligand, 2,2′-[(1,2-naphthalene)bis(oxy)]bis[N-(phenylmethyl)]acetamide (L) have been prepared and characterized by elemental analysis, conductivity measurements, IR and electronic spectroscopies. The crystal and molecular structures of the coordination polymer $\{[Eu_2L_3(Pic)_6]\cdot(CHCl_3)_3\cdot(H_2O)_{0.5}\}_n$ have been determined by single-crystal X-ray diffraction, and the structure displays a two-dimensional honeycomb-like framework in the *ab* plane, which can be regarded as a (6,3) topological network with europium atoms acting as “three-connected” centers. Furthermore, the coordination layers are linked by the intermolecular hydrogen bonds to form a three-dimensional (3-D) netlike supermolecule. Under excitation, Eu complex exhibited characteristic emissions. The lowest triplet state energy level of the ligand indicates that the triplet state energy level of the ligand matches better to the resonance level of Eu(III) than Tb(III) ion.

1. Introduction

Coordination polymers are presently playing a prominent role in material science [1] and their potential as functional materials is clearly recognized. The construction of supramolecular networks containing lanthanide ions as connectors is particularly attractive because of the electronic and magnetic properties of 4*f* ions, which should result in the application of lanthanide coordination polymers in sensors, lighting devices, and optical storage [2]. On the other hand, lanthanide ions, with their high coordination flexibility and their lack of preferential geometries, are good candidates to provide unique opportunities for the discovery of unusual network topologies [3–5], thus leading us to this interesting and challenging field. The number of lanthanide supramolecular structures is still very poor in contrast with that of transition metal supramolecular structures up to the present.

Since the *f*–*f* transitions are spin- and parity-forbidden, the excited state of the lanthanide ion is populated through intramolecular energy transfer from the ligand or ligands, which therefore serve as sensitizers (antenna effect) [6]. The role of the ligands is on the one hand to collect the photons provided by the light source in order to allow an energy transfer to the energy levels of the Ln(III) ion, and on the other hand to shield it against the solvent in order to avoid non-radioactive deactivation processes. It is generally accepted that the energy transfer from ligand to Ln(III) ion occurs from the lowest triplet state energy level (T_1) of the ligand to the resonance level of Ln(III) [7]. This energy transfer process is one of the most important processes having influence on the luminescent properties of the lanthanide complexes. Podand-type ligands have drawn much attention in recent years, mainly due to their selective coordinating capacity and hard binding sites, therefore, stabilizing their complexes, acquiring novel coordination structure and shielding the encapsulated ion from interaction with the surroundings [8]. Among numerous podands which have demonstrated their potential use in functional supramolecular chemistry [9], amide type podands are important for preparing the lanthanide complexes possessing strong luminescent properties.

Our group is interested in the supramolecular coordination chemistry of lanthanide ions with amide type podands that have strong coordination capability to the lanthanide ions and terminal group effects [10]. We have designed a series of amide type podands having both selective ability to coordinate lanthanide ions and enhanced luminescence of lanthanide complexes by providing some of proper conjugate absorption groups suitable for energy transfer [11]. In the present work, we designed and synthesized a new amide type podand ligand 2,2′-[(1,2-naphthalene)bis(oxy)]bis[N-(phenylmethyl)]acetamide (L) (Scheme 1) with two relatively long “arms”, and studied the crystal structure and luminescent properties of lanthanide complexes with this new ligand. The crystal structure of the complex $\{[Eu_2L_3(Pic)_6]\cdot(CHCl_3)_3\cdot(H_2O)_{0.5}\}_n$ unit shows that the Eu(III) ion

---

* Corresponding author. Fax: +869318912582.
E-mail address: tangyu@lzu.edu.cn (Y. Tang).

0022-4596/$ - see front matter © 2009 Elsevier Inc. All rights reserved.
doi:10.1016/j.jssc.2009.09.005

is coordinated with three oxygen atoms of the three ligands and six oxygen atoms of three bidentate picrates. At the same time, each ligand acts as an exo-bidentate linker and binds to two Eu^{3+} centers using its two carbonyl oxygen atoms of the amide groups. Six ligand linkers alternately bridge six $Eu(Pic)_3$ moieties to form a chairconformational hexagonal 66-membered ring, and the hexagonal rings are edgesharing to each other, yielding a two-dimensional (2-D) honeycomb-like framework, which can be regarded as a (6,3) topological network with europium atoms acting as "three-connected" nodes and $Eu(L)_{3/2}(Pic)_3$ units being regarded as repeating units. And the nitrogen atoms of the amide groups in the ligand arms are located in the outer part of the whole ligand molecule, which is very important for the assembly of the complex molecule units into a three-dimensional (3-D) netlike supermolecule by the intermolecular hydrogen bonds. Under excitation, Eu complex exhibited characteristic emissions. And the lowest triplet state energy level of the ligand which was calculated from the phosphorescence spectrum of the Gd complex at 77 K indicates that the triplet state energy level of the ligand matches better to the resonance level of Eu(III) than Tb(III) ion.

2. Experimental

2.1. Materials

Lanthanide picrates [12] and chloroacetobenzylamine [13] were prepared according to the literature methods. Other chemicals were obtained from commercial sources and used without further purification.

2.2. Chemical and physical measurements

Carbon, nitrogen and hydrogen were determined using an Elementar Vario EL (see Table 1). The IR spectra were recorded in the 4000–400 cm^{-1} region using KBr pellets and a Nicolet Nexus 670 FT-IR spectrometer (see Table 5). ^1H NMR spectra were measured on a Varian Mercury 300 spectrometer in $CDCl_3$ solutions, with TMS as internal standard. Electronic spectra were recorded with a Varian Cary 100 spectrophotometer in acetonitrile solution. Luminescence spectra and phosphorescence spectra were obtained on a Hitachi F-4500 fluorescence spectrophotometer. The quantum yield of the europium sample was determined by an absolute method using an integrating sphere (150 mm diameter, $BaSO_4$ coating) from Edinburgh Instruments FLS920. The lifetime measurement was measured on an Edinburgh Instruments FLS920 Fluorescence Spectrometer with Nd pumped OPOlette laser as the excitation source.

2.3. Crystal structure determination

X-ray diffraction data for a crystal of the europium complex with dimensions 0.45 mm × 0.32 mm × 0.13 mm were performed with graphite-monochromated Mo $K\alpha$ radiation on a Bruker CCD area-detector diffractometer and were collected by the ω–2θ scan technique. The crystal structure was solved by direct methods. All non-hydrogen atoms were refined anisotropically by full-matrix least-squares methods on F^2. Primary non-hydrogen atoms were solved by direct method and secondary non-hydrogen atoms were solved by difference maps. The hydrogen atoms were added geometrically and not refined. All calculations were performed using the programs SHELXS-97 and SHELXL-97 [14,15]. The crystal data and refinement results are summarized in Table 2. Selected bond lengths and angles are given in Table 3. CCDC reference number 737806.

2.4. Preparation of the ligand L

Chloroacetobenzylamine (3.20 g, 17.44 mmol) and naphthalene-2,3-diol (1.40 g, 8.73 mmol) were added to acetone (25 cm^3), then anhydrous potassium carbonate (1.20 g, 8.73 mmol) was added. The reaction mixture was stirred and refluxed for 5 h. After cooling down, the mixture was filtered and the solvent was distilled off. Then the resulted solid was recrystallized with acetone to get the ligand L; Yield: 73%. m.p.: 172–174 °C; ^1H NMR (d-$HCCl_3$, 300 MHz): 4.44(d, 4H), 4.65(s, 4H), 6.92(q, 2H), 7.17–7.71(m, 16H).

2.5. Preparation of the complexes

A solution of 0.15 mmol L in 10 cm^3 of chloroform was added drop wise to a solution of 0.1 mmol lanthanide picrates (Ln=Pr, Nd, Eu, Gd, Tb, Er) in 10 cm^3 of ethyl acetate. The mixture was stirred at room temperature for 4 h. Then the precipitated solid complex was filtered, washed with ethyl acetate and chloroform (V:V=1:1) and dried in vacuo over P_4O_{10} for 48 h and submitted

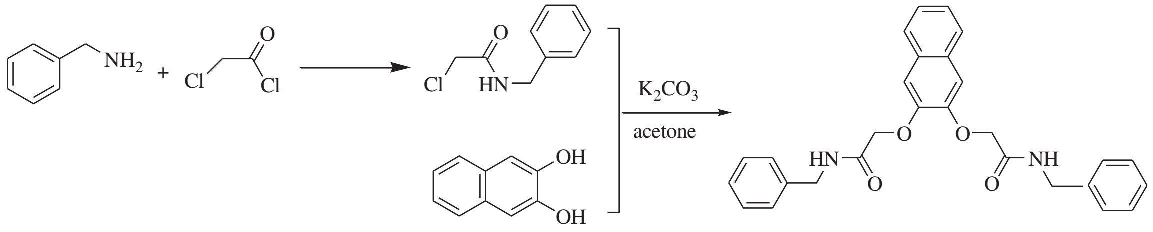

Scheme 1. The synthetic route for the ligand L.

Table 1
Analytical and molar conductance data of the complexes.

Complexes	%C found (Calc.)	%H found (Calc.)	%N found (Calc.)	Λ_m ($cm^2\,\Omega^{-1}\,mol^{-1}$)
$[Pr_2L_3(Pic)_6]\cdot(H_2O)_2$	47.32(47.26)	3.30(3.11)	11.21(11.02)	29.5
$[Nd_2L_3(Pic)_6]\cdot(H_2O)_2$	47.05(47.15)	3.03(3.10)	10.83(11.00)	29.8
$[Eu_2L_3(Pic)_6]\cdot(H_2O)_2$	47.03(46.92)	3.22(3.08)	11.05(10.94)	33.2
$[Gd_2L_3(Pic)_6]\cdot(H_2O)_2$	46.89(46.76)	3.15(3.07)	10.75(10.90)	33.0
$[Tb_2L_3(Pic)_6]\cdot(H_2O)_2$	46.67(46.70)	3.20(3.07)	10.55(10.89)	33.3
$[Er_2L_3(Pic)_6]\cdot(H_2O)_2$	46.81(46.45)	3.22(3.05)	10.55(10.83)	33.2

for elemental analysis. Yield: 60%. Analytical data and molar conductance values of the complexes are given in Table 1. All the complexes are yellow powders and stable in air. Single crystals of europium complex were grown from ethyl acetate and chloroform (V:V=1:1) mixed solution with slow evaporation at room temperature. After ca. 3 weeks, transparent yellow crystals were formed from the solution.

Table 2
Crystal data and structure refinement for the complex $\{[Eu_2L_3(Pic)_6]\cdot(CHCl_3)_3\cdot(H_2O)_{0.5}\}_n$.

Complex	$\{[Eu_2L_3(Pic)_6]\cdot(CHCl_3)_3\cdot(H_2O)_{0.5}\}_n$
Empirical formula	$C_{123}H_{94}Cl_9Eu_2N_{24}O_{54.5}$
Formula weight	3403.19
Temperature (K)	298(2) K
Wavelength (Å)	0.71073
Crystal system, Space group	Triclinic, $P-1$
a (Å)	20.543(2)
b (Å)	20.675(2)
c (Å)	21.760(3)
α (°)	110.215(2)
β (°)	99.8030(10)
γ (°)	115.295(2)
Volume (Å^3)	7269.9(14)
Z	2
$D_{calc.}$ (g cm^{-3})	1.555
μ (Mo $K\alpha$) (mm^{-1})	1.191
F(000)	3430
Crystal size (mm)	0.45 × 0.32 × 0.13
Range (deg.)	1.18–25.01
Index ranges	$-24 \le h \le 24$, $-24 \le k \le 23$, $-25 \le l \le 25$
Reflection collected	37685
Independent reflections	25254 [R(int)=0.0530]
Absorption correction	Semi-empirical from equivalents
Refinement method	Full-matrix least-squares on F^2
Data/restraints/parameters	25254/0/1982
Goodness-of-fit on F^2	1.021
Final R indices	R_1=0.0701, wR_2=0.1864
R indices (all data)	R_1=0.1413, wR_2=0.2386
Largest difference peak and hole (e Å^{-3})	1.520 and −1.150

3. Results and discussion

Analytical data for the newly synthesized complexes, listed in Table 1, indicate that the six complexes conform to a 2:3:6 metal-to-ligand-to-picrate stoichiometry $[Ln_2L_3(Pic)_6]\cdot(H_2O)_2$ (Ln=Pr, Nd, Eu, Gd, Tb, Er).

All the complexes are soluble in DMF, DMSO, methanol, ethanol, acetone, acetonitrile, THF, but slightly soluble in chloroform and ethyl ether. The molar conductances of the complexes in acetone (see Table 1) indicate that all complexes act as non-electrolytes [16], implying that all picrate groups are in coordination sphere.

3.1. *Crystal structure of* $\{[Eu_2L_3(Pic)_6]\cdot(CHCl_3)_3\cdot(H_2O)_{0.5}\}_n$

The single-crystal X-ray analysis of the complex $\{[Eu_2L_3(Pic)_6]\cdot(CHCl_3)_3\cdot(H_2O)_{0.5}\}_n$ reveals that the crystal crystallizes in triclinic space group $P-1$ and possesses a porous 2-D honeycomb open framework constructed from an extended array of trigonal-pyramidal Eu^{3+} centers and exo-bidentate ligands. The ligand molecules act as bridging linkers through their carbonyl oxygen atoms. The asymmetric unit in the complex contains two crystallographically independent Eu^{3+} centers. As shown in Fig. 1, the coordination sphere around each Eu^{3+} ion has a nine-coordinate environment, six of which are occupied by six oxygen atoms from three bidentate picrate groups, and the remaining three sites are occupied by the oxygen atoms of carbonyl groups of three separate ligands. The coordination environment of nine oxygen atoms around the Eu1 and Eu2 centers both can be described as distorted tricapped triprisms which have a slight difference (Fig. 2). At the same time, each ligand acts as an exo-bidentate

Table 3
Selected bond lengths (Å) and angles (°) for the complex $\{[Eu_2L_3(Pic)_6]\cdot(CHCl_3)_3\cdot(H_2O)_{0.5}\}_n$.

Eu(1)–O(27)	2.318(7)	Eu(1)–O(7)	2.341(7)	Eu(1)–O(13)	2.343(6)
Eu(1)–O(20)	2.354(7)	Eu(1)–O(11)	2.383(7)	Eu(1)–O(3)	2.385(6)
Eu(1)–O(14)	2.652(7)	Eu(1)–O(21)	2.672(8)	Eu(1)–O(28)	2.712(8)
Eu(2)–O(34)	2.320(7)	Eu(2)–O(48)	2.326(7)	Eu(2)–O(41)	2.334(7)
Eu(2)–O(12)	2.358(7)	Eu(2)–O(8)	2.408(6)	Eu(2)–O(4)	2.416(7)
Eu(2)–O(42)	2.615(7)	Eu(2)–O(49)	2.616(7)	Eu(2)–O(35)	2.617(7)
O(27)–Eu(1)–O(7)	131.9(2)	O(27)–Eu(1)–O(13)	79.1(2)	O(7)–Eu(1)–O(13)	142.6(2)
O(27)–Eu(1)–O(20)	140.5(2)	O(7)–Eu(1)–O(20)	82.0(2)	O(13)–Eu(1)–O(20)	81.0(3)
O(27)–Eu(1)–O(11)	79.4(2)	O(7)–Eu(1)–O(11)	86.5(2)	O(13)–Eu(1)–O(11)	79.1(2)
O(20)–Eu(1)–O(11)	129.3(2)	O(27)–Eu(1)–O(3)	81.8(2)	O(7)–Eu(1)–O(3)	80.9(2)
O(13)–Eu(1)–O(3)	130.4(2)	O(20)–Eu(1)–O(3)	85.7(2)	O(11)–Eu(1)–O(3)	140.6(2)
O(27)–Eu(1)–O(14)	69.8(2)	O(7)–Eu(1)–O(14)	137.8(2)	O(13)–Eu(1)–O(14)	64.8(2)
O(20)–Eu(1)–O(14)	70.9(2)	O(11)–Eu(1)–O(14	135.8(2)	O(3)–Eu(1)–O(14)	65.7(2)
O(27)–Eu(1)–O(21)	137.8(2)	O(7)–Eu(1)–O(21)	71.0(2)	O(13)–Eu(1)–O(21)	71.6(3)
O(20)–Eu(1)–O(21)	63.6(2)	O(11)–Eu(1)–O(21)	66.0(2)	O(3)–Eu(1)–O(21)	140.4(2)
O(14)–Eu(1)–O(21)	120.3(2)	O(27)–Eu(1)–O(28)	64.2(2)	O(7)–Eu(1)–O(28)	67.8(2)
O(13)–Eu(1)–O(28)	135.4(2)	O(20)–Eu(1)–O(28)	143.6(2)	O(11)–Eu(1)–O(28)	70.4(2)
O(3)–Eu(1)–O(28)	70.3(2)	O(14)–Eu(1)–O(28)	119.2(2)	O(21)–Eu(1)–O(28)	120.5(2)
O(34)–Eu(2)–O(48)	83.2(3)	O(34)–Eu(2)–O(41)	82.5(3)	O(48)–Eu(2)–O(41)	80.9(2)
O(34)–Eu(2)–O(12)	84.3(3)	O(48)–Eu(2)–O(12)	138.8(2)	O(41)–Eu(2)–O(12)	135.7(2)
O(34)–Eu(2)–O(8)	137.0(3)	O(48)–Eu(2)–O(8)	133.8(2)	O(41)–Eu(2)–O(8)	83.3(3)
O(12)–Eu(2)–O(8)	78.2(2)	O(34)–Eu(2)–O(4)	134.3(2)	O(48)–Eu(2)–O(4)	85.2(3)
O(41)–Eu(2)–O(4)	138.6(2)	O(12)–Eu(2)–O(4)	76.1(2)	O(8)–Eu(2)–O(4)	78.7(2)
O(34)–Eu(2)–O(42)	68.5(3)	O(48)–Eu(2)–O(42)	137.7(3)	O(41)–Eu(2)–O(42)	65.3(2)
O(12)–Eu(2)–O(42)	70.5(2)	O(8)–Eu(2)–O(42)	68.7(3)	O(4)–Eu(2)–O(42)	137.0(2)
O(34)–Eu(2)–O(49)	140.1(3)	O(48)–Eu(2)–O(49)	65.3(2)	O(41)–Eu(2)–O(49)	69.5(2)
O(12)–Eu(2)–O(49)	135.5(2)	O(8)–Eu(2)–O(49)	68.5(2)	O(4)–Eu(2)–O(49)	69.2(2)
O(42)–Eu(2)–O(49)	119.8(2)	O(34)–Eu(2)–O(35)	64.4(2)	O(48)–Eu(2)–O(35)	69.4(2)
O(41)–Eu(2)–O(35)	137.1(2)	O(12)–Eu(2)–O(35)	69.8(2)	O(8)–Eu(2)–O(35)	139.5(2)
O(4)–Eu(2)–O(35)	70.2(2)	O(42)–Eu(2)–O(35)	119.9(2)	O(49)–Eu(2)–O(35)	120.2(2)

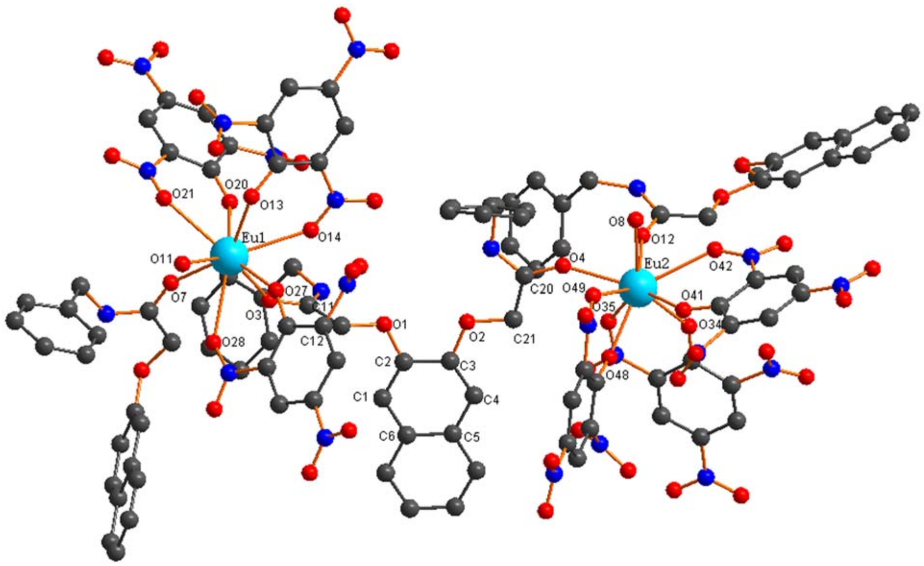

Fig. 1. Structure of $[Eu_2L_3(Pic)_6]$ showing the coordination sphere of Eu^{3+} along with atom labeling schemes. Hydrogen atoms and crystal lattice chloroform and water molecules are omitted for clarity.

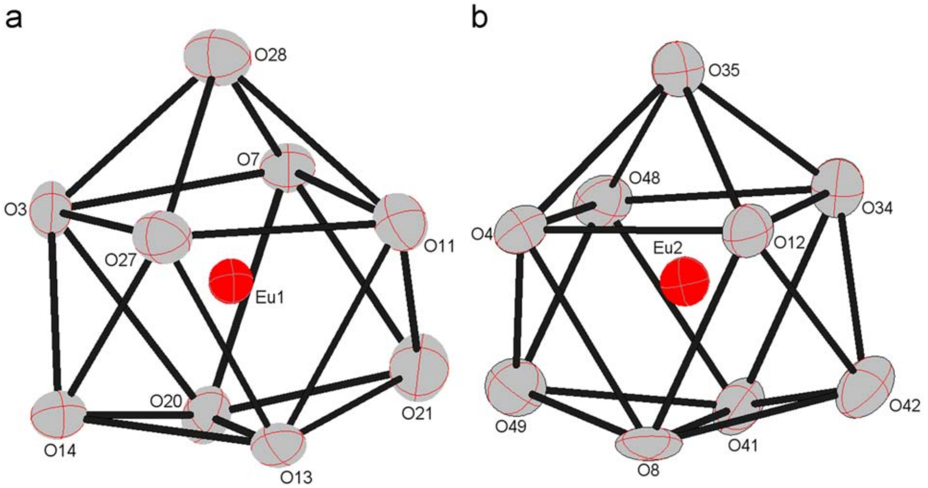

Fig. 2. Coordination polyhedron of Eu1 (a) and Eu2 (b) ions.

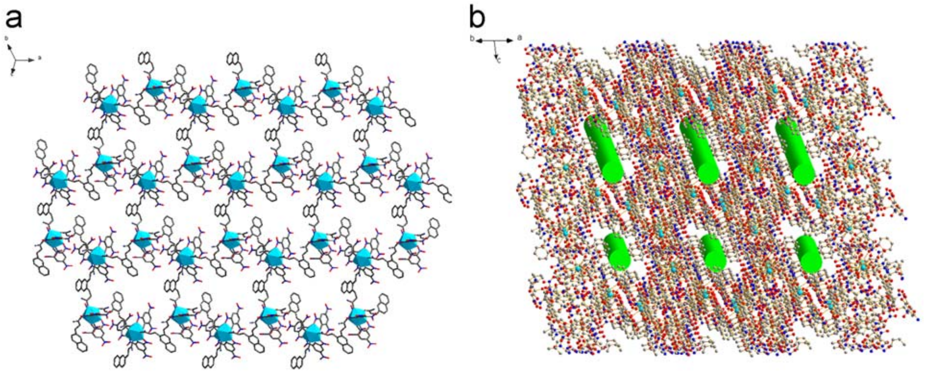

Fig. 3. (a) View of the 2-D honeycomb (6,3) topology network of the complex in the *ab* plane (the benzyl groups of the ligands, hydrogen atoms and crystalline chloroform and water molecules are omitted for clarity). (b) View of 2-D non-interpenetrating honeycomb-like layers of (6,3) topology with 1-D channels along the *c* axis. The green insets show the 1-D perforative column-like channels (hydrogen atoms as well as crystalline chloroform and water molecules are omitted for clarity).

linker and binds to two Eu^{3+} centers using its two carbonyl oxygen atoms of the amide groups. Thus, each ligand is coordinated to two Eu^{3+} and each Eu^{3+} is coordinated to three ligands to form a 3:2 (L:M) complex. Six ligand linkers alternately bridge six $Eu(Pic)_3$ moieties to form a hexagonal 66-membered ring, in which three non-adjacent Eu1 atoms are coplanar, paralleling the remaining three non-adjacent Eu2 atoms with a plane-to-plane distance of 4.509 Å. The hexagonal rings are edgesharing to each other, yielding a 2-D honeycomb-like framework in the *ab* plane (Fig. 3a), which can be regarded as a (6,3) topological network with europium atoms acting as "three-connected" nodes and $Eu(L)_{3/2}(Pic)_3$ units being regarded as repeating units. In the present case, the (6,3) net is not the ubiquitous flat graphene sheet but a topologically equivalent (6,3) net of chair conformation six-rings, which form a coordination polymer analogue of the puckered layers in graphite monofluoride, CF_x [17]. Furthermore, the corrugated honeycomb layers are stacked in an AAA manner along the *c* axis to produce a three-dimensional (3-D) hexagonal channel (Fig. 3b). The internal dimensions of the channel which have been evaluated taking into account the van der Waals radii of the involved atoms are about 8.5×13 Å. Calculations using PLATON [18] reveal that the solvent-accessible portion accounts for about 20% of the crystal volume. This dimension is sufficient to recognize suitable aromatic guest molecules such as toluene. The assembly of a honeycomb-like structure is challenging since the hexagon represents the most common pattern in nature and is familiar from benzene to the honeycomb of the bee. It is uncommon to generate honeycomb-like networks using the podand ligand. Especially, in this complex, the "all-chair" 2-D honeycomb network that is structurally analogous to CF_x is rare. To the best of our knowledge, this type of non-interpenerating neutral (6,3) topological framework constructed by linking flexible amide podands with lanthanide ions is very rare [19]. In addition, the coordination layers are linked by intermolecular hydrogen bonds O…H–N (listed in Table 4) to form a three-dimensional (3-D) netlike supermolecule. What greatly interests us here is that we find in this europium complex only oxygen atoms of carbonyl groups of the ligand take part in coordination with the metal ions, which shows the bridge type coordination polymer structure. And we also find the fact that all oxygen atoms chelate with the lanthanide ions in some kinds of amide-type podand ligands [20], and the metal ions could be effectively encapsulated and protected by the coordinated ligands. We may deduce that the skeleton, the resistance of the terminal groups of the ligands and the counter anions can all affect the molecular structure of the complexes.

Table 4
Hydrogen bonds in crystal packing (Å, °).

D–H…A	*d*(D–H)	*d*(H…A)	*d*(D…A)	∠DHA	Symmetry
N(1)–H(1)…O(38)	0.86	2.22	2.8721	133	$1-x,1-y,1-z$
N(3)–H(3)…O(52)	0.86	2.29	2.9280	131	$-x,1-y,1-z$
N(5)–H(5)…O(17)	0.86	2.47	3.2791	158	$-x,1-y,2-z$
N(6)–H(6)…O(17)	0.86	2.28	3.0607	151	$-x,1-y,2-z$

Table 5
The IR spectral data (cm^{-1}).

Compounds	ν(C=O)	ν(C–O–C)	ν(C–O)	$\nu_{as}(-NO_2)$	$\nu_s(-NO_2)$
HPic			1265s	1555m	1342s
L	1665	1168			
$[Pr_2L_3(Pic)_6]\cdot(H_2O)_2$	1615	1166	1268	1576, 1540	1362, 1330
$[Nd_2L_3(Pic)_6]\cdot(H_2O)_2$	1614	1167	1268	1576, 1538	1360, 1329
$[Eu_2L_3(Pic)_6]\cdot(H_2O)_2$	1616	1167	1269	1576, 1540	1363, 1331
$[Gd_2L_3(Pic)_6]\cdot(H_2O)_2$	1616	1168	1271	1576, 1540	1358, 1331
$[Tb_2L_3(Pic)_6]\cdot(H_2O)_2$	1614	1166	1269	1576, 1540	1365, 1330
$[Er_2L_3(Pic)_6]\cdot(H_2O)_2$	1614	1165	1269	1576, 1540	1363, 1331

3.2. *Infrared spectra*

The most important IR peaks of the ligand and the complexes $[Ln_2L_3(Pic)_6]\cdot(H_2O)_2$ are reported in Table 5.

The "free" ligand L exhibit two absorption bands at 1665 and 1168 cm^{-1} which are assigned to ν(C=O) and ν(C–O–C), respectively. In the complexes, the band of ether group remains almost unchanged, but the band for the carbonyl group red shifts to about 1615 cm^{-1} ($\Delta\nu$=50 cm^{-1}) as compared to the free ligand, thus indicating that only the oxygen atoms of the carbonyl group take part in coordination to the lanthanide ion. And this is in agreement with the crystal structure analysis.

The O–H out-of-plane bending vibration of the free HPic at 1151 cm^{-1} disappears, indicating that the H-atom of the O–H group is replaced by Ln(III). The vibration ν(C–O) of Pic^- at 1265 cm^{-1} is shifted toward higher frequency by ca. 3–6 cm^{-1} in the complexes. This is due to the following two effects. First, the hydrogen atom of the O–H group is replaced by Ln(III), increasing the π-bond character in the C–O bond. Secondly, coordination of the oxygen atom of L to Ln(III) decreases the π-character. The free HPic has $\nu_{as}(-NO_2)$ and $\nu_s(-NO_2)$ at 1555 and 1342 cm^{-1}, respectively, which split into two bands at ca. 1575, 1540 cm^{-1} and ca. 1360, 1330 cm^{-1}, respectively, in the complexes. This indicates that O-atoms in the nitro group of Pic^- take part in coordination [21]. Additionally, broad bands at 3400 cm^{-1} could be attributed to the O–H stretching vibrations of water molecules.

3.3. *Electronic spectra*

The electronic spectra in the visible region of the Ln(III) complexes exhibit alternations in intensity and shifts in position of the absorption bands relative to the corresponding Ln(III) aquo ions. The shift has been attributed by Jørgensen to the effect on the crystal field of interelectronic repulsion between the 4*f* electrons, and is related to the covalent character of the metal–ligand bond, assessed by Sinha's parameter (δ), the nephelauxetic ration (β) and the bonding parameter ($b^{1/2}$) [22], where β is the average value of the ratio V_c/V_a taking into account as many transitions as possible (V_c and V_a are wavenumber of complex and

Table 6
Electronic spectral data and covalent parameters of Nd and Er complexes.

Complexes	Frequency (cm^{-1})	Assignment	Covalent parameters
$[Nd_2L_3(Pic)_6]\cdot(H_2O)_2$	12500(12608)	${}^4I_{9/2}\rightarrow{}^2H_{9/2}$	β=0.9934
	13441(13435)	${}^4I_{9/2}\rightarrow{}^4S_{3/2}$	δ=0.6644
	17182(17203)	${}^4I_{9/2}\rightarrow{}^2G_{7/2}$	$B^{1/2}$=0.0574
	19084(19414)	${}^4I_{9/2}\rightarrow{}^4G_{9/2}$	
$[Er_2L_3(Pic)_6]\cdot(H_2O)_2$	15385(15136)	${}^4I_{15/2}\rightarrow{}^4F_{9/2}$	β=1.0094
	19194(19147)	${}^4I_{15/2}\rightarrow{}^2H_{11/2}$	$\delta=-0.9312$

aquo ion). Depending upon the ligands, the values of δ may either be positive (covalent bonding) or negative (ionic bonding). Although the absolute values of δ are of less importance, they may be conveniently used in assessing the relative covalent character of the complexes. The energy of a given transition depends critically on the interelectronic repulsion terms of the Hamiltonian, which, for equivalent 4f electrons, give rise to the Slater integrals.

Absorption spectra of the Nd(III) and Er(III) complexes were registered in acetonitrile solution at room temperature and the covalent parameters were calculated (Table 6). The values of β, which are less than unity, and positive values of δ and $b^{1/2}$ of the Nd^{3+} complex indicate that the metal–ligand bonds present some covalent character [23]. And the β value for Er(III) complex is more than unity and δ value is negative suggesting that Er^{3+}–O bond of the complex has weaker covalency than that of Er^{3+} aquo ion.

3.4. Luminescent properties of the complexes

Monitored by the emission band at 615 nm, the europium complex exhibits broad excitation bands around 400 nm. The luminescence emission spectra of the ligand L and the europium complex in solid state (the excitation and emission slit widths were 2.5 and 5.0 nm respectively, Fig. 4a) and in acetone, acetonitrile, methanol and ethanol solutions (concentration: 1.0×10^{-3} mol L^{-1}, the excitation and emission slit widths were 5.0 nm, Fig. 4b) were recorded at room temperature. It can be seen from Fig. 4a that the Eu complex shows the characteristic *f–f* transition emissions of Eu^{3+} when excited with 408 nm in the solid state. This indicates that the ligand L is a comparative good organic chelator to absorb energy and transfer them to Eu ion. The intensity ratio of the $^5D_0\to{}^7F_2$ transition to the $^5D_0\to{}^7F_1$ transition is widely used as a measure of the coordination state and the site symmetry of the europium ion, since the $^5D_0\to{}^7F_1$ emission is independent of the ligand environment, and primarily magnetic dipole in character, while the $^5D_0\to{}^7F_2$ emission is essentially purely electric dipole in character, and its intensity is very sensitive to the crystal field symmetry. In the spectrum of the complex, the most intensity ratio value $\eta(^5D_0\to{}^7F_2/^5D_0\to{}^7F_1)$ is 5.8 (Table 7), showing that the Eu(III) ion does not lie in a centrosymmetric coordination site [24], in agreement with the crystal structure analysis.

Table 7
Luminescence data for the Eu complex in solid state and in different solutions at room temperature.

Solvent	λ_{Ex} (nm)	λ_{Em} (nm)	RFI^a	Assignments
Solid state	408	578.2	2.580	$^5D_0\to{}^7F_0$
		588.8	7.473	$^5D_0\to{}^7F_1$
		615.0	43.49	$^5D_0\to{}^7F_2$
Acetone	463	578.8	12.05	$^5D_0\to{}^7F_0$
		592.0	16.35	$^5D_0\to{}^7F_1$
		613.4	47.00	$^5D_0\to{}^7F_2$
Acetonitrile	464	578.4	10.12	$^5D_0\to{}^7F_0$
		591.0	8.912	$^5D_0\to{}^7F_1$
		613.6	32.40	$^5D_0\to{}^7F_2$
Methanol	460	577.8	8.445	$^5D_0\to{}^7F_0$
		594.2	8.680	$^5D_0\to{}^7F_1$
		613.2	9.100	$^5D_0\to{}^7F_2$
Ethanol	465	613.2	7.520	$^5D_0\to{}^7F_2$

RFI^a: relative fluorescence intensity.

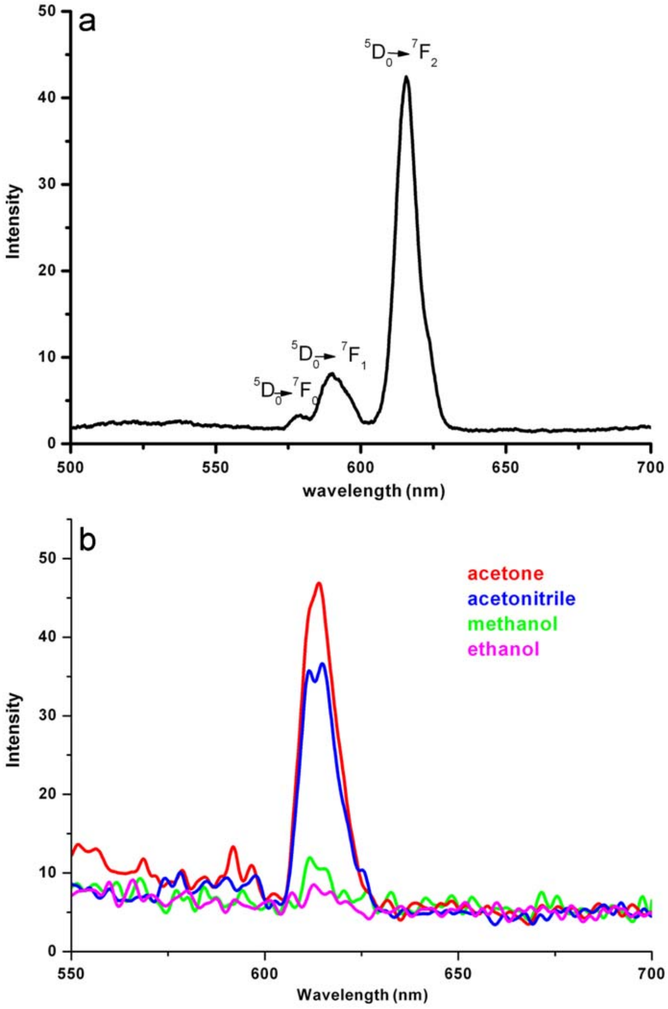

Fig. 4. Emission spectra of the Eu complex: (a) solid state; (b) in different solutions at room temperature.

An intramolecular energy transfer from the triplet state of the ligand to the resonance level of the Ln(III) ion is one of the most important processes having influence on the Ln(III) luminescent properties of Ln(III) chelates [7b]. A triplet excited state T_1 which is localized on one ligand only and is independent of the rare earth nature [7b]. In order to acquire the triplet excited state T_1 of the ligand L, the phosphorescence spectrum of the Gd(III) complex was measured at 77 K in a methanol–ethanol mixture (V:V=1:1). The triplet state energy level T_1 of the ligand L, which was calculated from the shortest-wavelength phosphorescence band [7a], is 21993 cm^{-1}. This energy level is above the lowest excited resonance level $^5D_0$ of Eu(III) (17300 cm^{-1}) and $^5D_4$ (20500 cm^{-1}) of Tb(III). Thus, the absorbed energy could be transferred from ligand to the Eu or Tb ions. And we may deduce that the triplet state energy level T_1 of this ligand L matches better to the lowest resonance level of Eu(III) (Δv=4693 cm^{-1}) than Tb(III) (Δv=1493 cm^{-1}) ion, because such small Δv (T_1–$^5D_4$) could result in the non-radioactive deactivation of the terbium emitting state via a back-energy transfer process ($T_1\leftarrow$Tb($^5D_4$)) and quench the luminescence of the Tb complex [7c]. Actually, we do not observe the characteristic fluorescence of the Tb(III) complex at room temperature which is entirely consistent with the observed efficient quenching of emission by the back-energy transfer process. The fluorescence quantum yield Φ of the europium picrate complex in solid state was found to be 0.56 ± 0.1% using an integrating sphere. And the Eu(III) complex luminescence decay is best described by a single-exponential process with significantly longer lifetimes of τ=0.194 ± 0.001 ms, indicating the presence of one distinct emitting species.

It could be seen from Fig. 4b that in acetone solution the Eu complex has the strongest luminescence, and then in acetonitrile, methanol and ethanol. This is due to the coordinating effects of solvents, namely solvate effect [25]. Together with the raising coordination abilities of acetone, acetonitrile, methanol, and ethanol for the lanthanide ions, the oscillatory motions of the entering molecules consume more energy which the ligand triplet level transfer to the emitting level of the lanthanide ion. Thus, the energy transfer could not be carried out perfectly.

4. Conclusions

In summary, six new lanthanide picrate complexes $[Ln_2L_3(Pic)_6]\cdot(H_2O)_2$ (Ln=Pr, Nd, Eu, Gd, Tb, Er) of an amide type podand ligand 2,2′-[(1,2-naphthalene)bis(oxy)]bis[N-(phenylmethyl)]acetamide (L) were obtained and structurally characterized. The crystal and molecular structures of the coordination polymer $\{[Eu_2L_3(Pic)_6]\cdot(CHCl_3)_3\cdot(H_2O)_{0.5}\}_n$ display a two-dimensional honeycomb-like framework in the *ab* plane, which can be regarded as a (6,3) topological network with europium atoms acting as "three-connected" centers. We deduce that there may be two reasons for the interesting results. Firstly, the semirigid bis-monodentate nature of the ligand makes it easy to bind to two Ln(III) ions using its two oxygen atoms of the amide groups. This is one of the key triggers for the construction of the backbone of the 2-D coordination polymers. The other reason, Pic^-, as a suitable counter ion was chosen. The coordination number provided by the bridging ligands is only three, which is not sufficient for high coordinated lanthanide ions. An additional three bidentate picrates make the total coordinated number nine, satisfying the need of high coordination number. The luminescent properties of the Eu(III) complex in solid state and different solutions were investigated. Under the excitation of UV light, the complex exhibited characteristic emission of central metal ions. And the lowest triplet state energy level of the ligand indicates that the triplet state energy level of the ligand matches better to the resonance level of Eu(III). To sum up, we designed a new bridging podand ligand with semirigid skeleton and two long arms, which can strongly bind Ln(III) ions to form elegant coordination polymeric architectures and sensitize Eu(III) luminescence emission. From a more general outlook, the coupling of coordination polymer and luminescence in a material has interesting prospects for the development of lanthanide complex luminescent materials.

5. Supplementary material

Crystallographic data for the structural analysis have been deposited with the Cambridge Crystallographic Data Center, CCDC no. 737806. Copies of this information may be obtained free of charge from the director, CCDC, 12 Union Road, Cambridge CB2 IEZ, UK (e-mail: deposit@ccdc.cam.ac.uk or www: http://www.ccdc.cam.ac.uk).

Acknowledgments

This work was supported by the National Natural Science Foundation of China (Project 20401008) and the program for New Century Excellent Talents in University (NCET-06-0902) for financial support.

Appendix A. Supplementary material

Supplementary data associated with this article can be found in the online version at doi:10.1016/j.jssc.2009.09.005.

References

[1] S. Kitagawa, S. Noro, Comprehensive Coordination Chemistry II, vol. 3, Elsevier Ltd., Oxford, UK, 2004;
C. Janiak, Dalton Trans. (2003) 2781.
[2] [a] K. Kuriki, Y. Koike, Y. Okamoto, Chem. Rev. 102 (2002) 2347;
[b] C.L. Cahill, D.T. De Lill, M. Frisch, Cryst. Eng. Commun. 9 (2007) 15;
[c] K.A. Gschneidner Jr., V. Pecharsky, J.-C.G. Bünzli, O. Guillou, C. Daiguebonne, Handbook on the Physics and Chemistry of Rare Earths, vol. 34, Elsevier, Amsterdam, The Netherlands, 2005;
[d] R.J. Hill, D.L. Long, P. Hubberstey, M. Schröder, N.R. Champness, J. Solid State Chem. 178 (2005) 2414;
[e] J.-C.G. Bünzli, C. Piguet, Chem. Soc. Rev. 34 (2005) 1048;
[f] A.Y. Robin, K.M. Fromm, Coord. Chem. Rev. 250 (2006) 2127;
[g] S. Faulkner, J.L. Matthews, Comprehensive Coordination Chemistry II, vol. 9, Elsevier, Oxford, UK, 2004, p. 913;
[h] C. Piguet, J.C.G. Bünzli, Chem. Soc. Rev. 28 (1999) 347;
[i] R. Gheorghe, P. Cucos, M. Andruh, J.P. Costes, B. Donnadieu, S. Shova, Chem. Eur. J. 12 (2005) 187.
[3] [a] W.-S. Liu, T.-Q. Jiao, Y.-Z. Li, Q.-Z. Liu, M.-Y. Tan, H. Wang, L.-F. Wang, J. Am. Chem. Soc. 126 (2004) 2280;
[b] B.-Q. Ma, D.-S. Zhang, S. Gao, T.-Z. Jin, C.-H. Yan, G.-X. Xu, Angew. Chem. Int. Ed. 39 (2000) 3644;
[c] C. Serre, N. Stock, T. Bein, G. Férey, Inorg. Chem. 43 (2004) 3159.
[4] [a] G. Mancino, A.J. Ferguson, A. Beeby, N.J. Long, T.S. Jones, J. Am. Chem. Soc. 127 (2005) 524;
[b] T.M. Reineke, M. Eddaoudi, M. Fehr, D. Kelley, O.M. Yaghi, J. Am. Chem. Soc. 121 (1999) 1651;
[c] X. Guo, G. Zhu, Q. Fang, M. Xue, G. Tian, J. Sun, X. Li, S. Qiu, Inorg. Chem. 44 (2005) 3850.
[5] [a] F. Luo, Y.-X. Che, J.-M. Zheng, Cryst. Growth Des. 6 (2006) 2432;
[b] D.-X. Hu, F. Luo, Y.-X. Che, J.-M. Zheng, Cryst. Growth Des. 7 (2007) 1733.
[6] [a] G.F. Desa, O.L. Malta, C. De Mello Donega, A.M. Simas, R.L. Longo, P.A. Santa-cruz, E.F. da Silva Jr., Coord. Chem. Rev. 196 (2000) 165;
[b] C. Bazzicalupi, A. Bencini, A. Bianchi, C. Ciorgi, V. Fusi, A. Masotti B. Valtancoli, A. Roque, F. Pina, Chem. Commun. 7 (2000) 561.
[7] [a] W. Dawson, J. Kropp, M. Windsor, J. Chem. Phys. 45 (1966) 2410;
[b] M. Latva, H. Takalob, V.M. Mukkala, C. Matachescuc, J.C. Rodriguez-Ubisd, J. Kankarea, J. Lumin. 75 (1997) 149;
[c] F. Gutierrez, C. Tedeschi, L. Maron, J.P. Daudey, R. Poteau, J. Azema, P. Tisnès, C. Picard, J. Chem. Soc. Dalton Trans. (2004) 1334.
[8] [a] F. Renaud, C. Piguet, G. Bernardinelli, J.-C.G. Bunzli, G. Hopfgartner, J. Am. Chem. Soc. 121 (1999) 9326;
[b] L.H. Gade, Acc. Chem. Res. 35 (2002) 575;
[c] C.S. Hamann, A.V. Zelewsky, A. Barbieri, F. Barigelletti, G. Muller, J.P. Riehl, A. Neels, J. Am. Chem. Soc. 126 (2004) 9339.
[9] [a] C.-Y. Su, Y.-P. Cai, C.-L. Chen, M.D. Smith, W. Kaim, H.C. zur Loye, J. Am. Chem. Soc. 125 (2003) 8595;
[b] C.-Y. Su, Y.-P. Cai, C.-L. Chen, F. Lissner, B.S. Kang, W. Kaim, Angew. Chem., Int. Ed. Engl. 41 (2002) 3371.
[10] B. Tümmler, G. Maass, F. Vögtle, J. Am. Chem. Soc. 101 (1979) 2588.
[11] [a] J. Zhang, Y. Tang, N. Tang, M.-Y. Tan, W.-S. Liu, K.-B. Yu, J. Chem. Soc. Dalton Trans. (2002) 832;
[b] Z.-H. Cai, Y. Tang, W.-S. Liu, M.-Y. Tan, Chem. Lett. 3 (2004) 342;
[c] Y. Tang, J. Zhang, W.-S. Liu, M.-Y. Tan, K.-B. Yu, Polyhedron 24 (2005) 1160.
[12] Y.-C. Tian, Y.-Q. Liang, J.-Z. Ni, China Univ. Chem. J. 9 (1988) 113.
[13] W. Baker, K.M. Buggle, J.F.W. McOmie, D.A.M. Watkins, J. Chem. Soc. (1958) 3594.
[14] G.M. Sheldrick, Acta Crystallogr. A 46 (1990) 467.
[15] G.M. Sheldrick, SHELXS-97, A Program for X-ray Crystal Structure Solution, and SHELXL-97, A Program for X-ray Structure Refinement, Gottingen University, Germany, 1997.
[16] W.J. Geary, Coord. Chem. Rev. 7 (1971) 81.
[17] [a] T.J. Prior, M.J. Rosseinsky, Chem. Commun. (2001) 495;
[b] Y.-L. Wang, D.-Q. Yuan, W.-H. Bi, X. Li, X.-J. Li, F. Li, R. Cao, Cryst. Growth Des. 5 (2005) 1849.
[18] A. Spek, L *PLATON*, Utrecht University, Utrecht, The Netherlands, 2003.
[19] Y.-L. Guo, W. Dou, X.-Y. Zhou, W.-S. Liu, W.-W. Qin, Z.-P. Zang, J.-R. Zhang D.-Q. Wang, Inorg. Chem. 48 (2009) 3581.
[20] Y. Tang, K.-Z. Tang, J. Zhang, C.-Y. Su, W.-S. Liu, M.-Y. Tan, Inorg. Chem. Commun. 8 (2005) 1018.
[21] S.-X. Liu, W.-S. Liu, M.-Y. Tan, K.-B. Yu, J. Coord. Chem. 10 (1996) 391.
[22] [a] C.K. Jørgenson, Prog. Inorg. Chem. 4 (1962) 73;
[b] S.P. Sinha, Spectrochim. Acta 22 (1966) 57;
[c] D.E. Henrie, G.R. Choppin, J. Chem. Phys. 49 (1968) 477.
[23] A.K. Solanki, A.M. Bhandaka, J. Inorg. Nucl. Chem. 41 (1979) 1311.
[24] M. Albin, R.R. Wright Jr., W.D. Horrocks, Inorg. Chem. 24 (1985) 2491.
[25] H.-Q. Liu, T.-C. Cheung, C.-M. Che, Chem. Commun. (1996) 1039.